

**Ab initio study of structural stability, elastic, vibrational, and electronic properties of TiPd<sub>2</sub>**Xing-Qiu Chen,<sup>1,2,\*</sup> Walter Wolf,<sup>3</sup> Raimund Podlucky,<sup>1</sup> and Peter Rogl<sup>1</sup><sup>1</sup>Department of Physical Chemistry, University of Vienna, Sensengasse 8/7, A 1090 Vienna, Austria<sup>2</sup>School of Materials and Metallurgy, Northeastern University, Shenyang 110004, People's Republic of China<sup>3</sup>Materials Design S.A.R.L., 44, Avenida F.-A. Bartholdi, 72000 Le Mans, France

(Received 4 May 2007; revised manuscript received 26 July 2007; published 10 September 2007)

By means of a density functional theory approach, we calculated the structural stabilities, electronic structure, elastic constants, and vibrational properties of the compound TiPd<sub>2</sub>. The results indicate that the tetragonal MoSi<sub>2</sub>-type (*C11<sub>b</sub>*) structure is unstable, whereas the orthorhombically distorted MoPt<sub>2</sub>-type (*oI6*) structure is the stable ground state phase. Thermodynamical properties such as enthalpies of formation, zero-point energies, and temperature-dependent free energies were calculated. A phase transition from the orthorhombic ground state to the *C11<sub>b</sub>* structure was derived for about 1000 K, in reasonable agreement with the most recent experiment. According to our results, the tetragonal-to-orthorhombic structural transition is driven by vibrational entropy.

DOI: 10.1103/PhysRevB.76.092102

PACS number(s): 61.50.Ah, 61.50.Ks, 62.50.+p, 62.20.Qp

Ti-Pd intermetallic compounds are of interest for applications in engineering and medicine because of their mechanical and structural shape memory properties.<sup>1-3</sup> Furthermore, some of the compounds are of interest for the reversible storage of hydrogen.<sup>4</sup> Ti<sub>2</sub>Pd is known for its hydrogen absorption capabilities,<sup>5</sup> whereas for TiPd<sub>2</sub>, this property still needs to be proven, as has recently been discussed for the corresponding Zr compounds.<sup>6</sup>

In spite of its technological interest, the structural stability of TiPd<sub>2</sub> is still under debate. Recent perturbed angular correlation experiments by Wodniecki *et al.*<sup>7</sup> found an orthorhombically distorted variant of the tetragonal *C11<sub>b</sub>* structure which appeared in a wide temperature range from 24 to 1023 K. This result agrees with a rather early investigation,<sup>8</sup> but is in contradiction to the latest Ti-Pd phase diagram.<sup>9</sup> There, it is reported that TiPd<sub>2</sub> prefers the *C11<sub>b</sub>* structure below 1553 K, whereas at higher temperatures up to 1673 K, an orthorhombic variant gets stabilized. Until now, the competition of the tetragonal *C11<sub>b</sub>* structure with orthorhombically distorted variants is not understood, and more detailed structural information (such as space group and atomic sites) is missing. In addition, very little is known about important material parameters, which, of course, depend on the crystal structure. Because of this general lack of information and the unresolved phase stability, *ab initio* density functional calculations for TiPd<sub>2</sub> are certainly able to help fill this gap. Therefore, we performed such investigations and derived structural stabilities, elastic constants, and phonon dispersions, and we analyzed the electronic structure of relevant phases. The temperature dependence of the structural stability was derived from the vibrational free energy. On the basis of our results, we believe that the structural stability of TiPd<sub>2</sub> is now understood, as we will elaborate in this Brief Report.

For the density functional theory (DFT) calculations, we applied the Vienna *ab initio* simulation package<sup>10</sup> (VASP) with the projector augmented wave potential<sup>11,12</sup> construction. An energy cutoff of 400 eV was chosen. For the exchange-correlation functional, the generalized gradient approximation of Perdew and Wang<sup>13</sup> was taken. The Brillouin zone integrations were performed for suitably large sets of  $\vec{k}$

points according to Monkhorst and Pack.<sup>14</sup> For geometry optimizations and elastic constants,  $11 \times 11 \times 9$  and  $11 \times 13 \times 9$  meshes for *C11<sub>b</sub>* and *oI6*, respectively, and for the 54 atom supercells for phonon calculations,  $3 \times 3 \times 3$  meshes were applied. Optimization of structural parameters (atomic positions and lattice parameters) was achieved by minimization of forces and stress tensors. The phonon dispersions and phonon densities of states for both the tetragonal *C11<sub>b</sub>* and orthorhombic *oI6* structures were calculated in the framework of the direct method,<sup>15,16</sup> for which the force

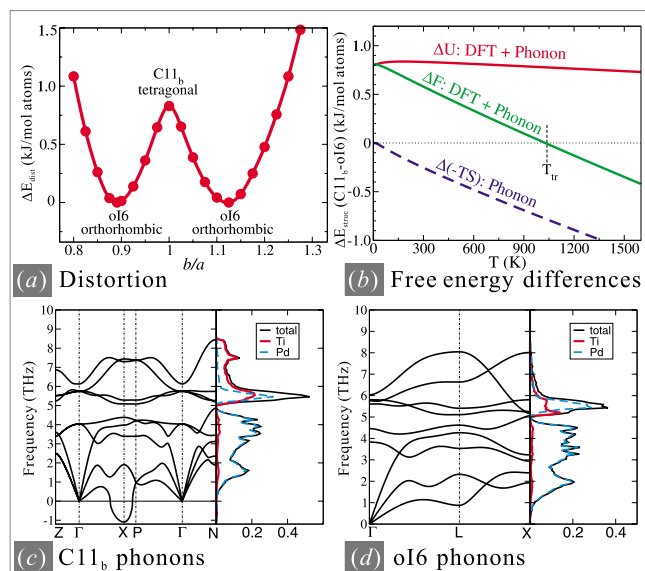


FIG. 1. (Color online) (a) The energy of distortion  $\Delta E_{\text{dist}}$  (relative to the minima) of the tetragonal *C11<sub>b</sub>* TiPd<sub>2</sub> phase as a function of  $b/a$  at its equilibrium volume. (b) Calculated temperature-dependent energy differences  $\Delta E_{\text{struc}}$  between the *C11<sub>b</sub>* and *oI6* structures: total free energy ( $\Delta F$ ), internal energy ( $\Delta U$  including enthalpies of formation and zero-point energies), and entropy  $[-T\Delta(S)]$  including DFT and phonon contributions. [(c) and (d)] *Ab initio* phonon dispersion and phonon density of states [total PDOS in unit of states/(THz f.u.); partial PDOS in unit of states/(THz atom)] for the *C11<sub>b</sub>* and *oI6* structures of TiPd<sub>2</sub>.

TABLE I. Structural parameters and enthalpies of formation  $\Delta H$  of  $\text{TiPd}_2$ : *ab initio* predictions (this work) and experimental data.

Structure	$a$ (Å)	$b$ (Å)	$c$ (Å)	$\Delta H$ (kJ/mol of atoms)
C40	4.833		6.885	-57.2
C49	3.569	12.609	4.115	-59.3
$C11_b$	3.271		8.751	-60.8
	3.24 <sup>a</sup>		8.48 <sup>a</sup>	
$oI6$	3.456	3.097	8.729	-61.6
	3.41 <sup>a</sup>	3.07 <sup>a</sup>	8.56 <sup>a</sup>	-58.1±1.3 <sup>b</sup>

<sup>a</sup>Reference 8.

<sup>b</sup>Reference 25.

constants were derived by a supercell approach with VASP (as in Ref. 17). Their elastic constants were calculated from total energies as a function of suitably selected distortions (see Refs. 17 and 18 for details).

In a first step, the lattice parameters and atom positions of the tetragonal  $C11_b$  structure were optimized. Then we searched for possible ground state orthorhombic structures for  $\text{TiPd}_2$  by distortion of the  $ab$  plane of the equilibrium  $C11_b$  unit cell, keeping both  $c$  and volume fixed and simultaneously allowing all free atomic parameters to fully relax. The energy of distortion as a function of the  $b/a$  ratio is compiled in Fig. 1(a). The plot gives two important pieces of information: (1) there is a maximum at  $b/a=1$ , indicating that the tetragonal  $C11_b$  phase is unstable against orthorhombic deformation; (2) the curve has two equally deep minima at  $b/a=0.891$  and  $1.124$ , respectively. In fact, these two minima correspond to the identical orthorhombic structure  $oI6$  ( $\text{MoPt}_2$  type,  $Immm$ , No. 71). Comparing to the tetragonal  $C11_b$  structure in Table I, the obtained  $oI6$  structure exhibits two main differences: (1)  $a$  is not equal to  $b$  in  $oI6$ , and (2) the  $4i$  site (0, 0, 0.3422) of Pd replaces the  $4e$  site (0, 0, 0.3431) in the  $C11_b$  structure. Two other related structures (C40 and C49) were further considered. Among all these structures, the  $oI6$  phase is still the lowest in energy and  $C11_b$  is the second most stable phase. It is worth emphasizing that all these phases are found to have almost the same equilibrium volume. Table I demonstrates that the calculated lattice constants are in good agreement with experiments, which is particularly true for  $a$  and  $b$  parameters. The  $c$  parameter of the  $oI6$  phase is 2% and that of the tetragonal  $C11_b$  phase is 3% larger than experiment. We attributed this deviation to the generalized gradient approximation to exchange and correlation that is known for its tendency to overestimate lattice parameters and also introduce inaccuracies in relative lattice spacings.

TABLE II. Calculated elastic constants (GPa) of  $\text{TiPd}_2$ . The bulk moduli derived from the elastic constants are in good agreement with the values (in parentheses) obtained from a fit to the energy-volume curves.

Phase	$c_{11}$	$c_{12}$	$c_{13}$	$c_{22}$	$c_{23}$	$c_{33}$	$c_{44}$	$c_{55}$	$c_{66}$	$B_0$
$\text{TiPd}_2$ ( $C11_b$ )	128.8	195.1	121.4			221.4	72.0		99.7	150.5 (152.3)
$\text{TiPd}_2$ ( $oI6$ )	214.7	121.7	167.7	201.7	72.7	229.1	62.1	81.4	95.5	152.1 (153.3)

The calculated elastic constants of the low-energy  $C11_b$  and  $oI6$  phases are compiled in Table II. For both structures, all elastic constants are positive; however, for the  $C11_b$  structure, the linear combination  $c_{11}-c_{12}$  amounts to  $-66.3$  GPa. This strongly negative value disobeys the stability criteria for tetragonal structures<sup>23</sup> and indicates spontaneous deformation toward an orthorhombic structure to lower the energy, as has, indeed, been observed in Fig. 1(a). In contrast, the nine independent elastic constants of the orthorhombic  $oI6$  structure (Table II) clearly obey the corresponding stability criteria for orthorhombic lattices.<sup>23,24</sup>

The computed phonon dispersions and the phonon densities of states (PDOS) of the  $C11_b$  and  $oI6$  phases at their equilibrium volumes are shown in Figs. 1(c) and 1(d). For tetragonal  $C11_b$ , a mode with imaginary frequencies in a small area of reciprocal space centered around point X is observed, indicating a vibrational instability. On the other hand, for orthorhombic  $oI6$ , all phonon branches exhibit real frequencies in the entire Brillouin zone, characteristic of a vibrationally stable structure. As can be seen in Figs. 1(c) and 1(d), the positive PDOS looks similar for  $C11_b$  and  $oI6$ . Three well separated bands can be distinguished. The modes below 5 THz are mainly due to vibrations of Pd atoms. Vibrations of both Pd and Ti atoms contribute to the modes between 5 and 6 THz. At high frequencies above 6 THz, the spectrum is dominated by Ti atom vibrations.

Temperature-dependent thermodynamic functions were derived from the total electronic energy ( $U_{\text{DFT}}$ ) and the PDOS: (i) The zero-temperature enthalpy of formation was calculated as the difference in total energies of the compound and the constituent elements in their ground state phases:  $\Delta H = \frac{1}{3}[U_{\text{DFT}}(\text{TiPd}_2) - U_{\text{DFT}}(\text{Ti}) - 2U_{\text{DFT}}(\text{Pd})]$ .<sup>19</sup> The calculated enthalpy of formation of the most stable  $oI6$  phase is  $-61.58$  kJ (mol of atoms)<sup>-1</sup> (Table I), agreeing very well with the measured calorimetric data<sup>25</sup> at 298 K [ $-58.1 \pm 1.3$  kJ (mol of atoms)<sup>-1</sup>]. (ii) The zero-point energies  $E_{0,\text{vib}}$  as derived from the PDOS<sup>20</sup> are very similar, amounting to 2.60 and 2.67 kJ (mol of atoms)<sup>-1</sup> for  $C11_b$  and  $oI6$ , respectively, slightly reducing their structural energy difference to 0.80 kJ (mol of atoms)<sup>-1</sup> at 0 K. (iii) Finally, the temperature-dependent phonon free energy ( $F_{\text{ph}}$ ), internal energy, and entropy are derived from the PDOS.<sup>17,21,22</sup> The contribution of the soft mode with imaginary frequencies to the thermodynamic functions of the  $C11_b$  phase has been ignored. This contribution to the free energy is expected to be quite small according to Ref. 26, because the barrier of the double well responsible for the instability is only 0.8 kJ (mol of atoms)<sup>-1</sup>, as illustrated in Fig. 1(a). For a quantitative estimation of this error, we lifted the soft mode at X into the real spectrum by manipulation of the force constants related to this mode, thereby removing the imagi-

nary frequencies. At 1000 K, the free energy was lowered by less than  $0.2 \text{ kJ} (\text{mol of atoms})^{-1}$ , thus decreasing the transition temperature discussed below by about 150 K.

Combining these three contributions, the total temperature-dependent free energy is expressed as  $F = \Delta H + E_{0,vib} + F_{ph}$ . The difference between the total free energies of  $C11_b$  and  $oI6$   $\Delta F = F_{C11_b} - F_{oI6}$  is displayed in Fig. 1(b). A structural phase transition occurs from  $oI6$ , stable at low temperatures, to  $C11_b$  at the transition temperature  $T_{tr} \approx 1100 \text{ K}$ . Including the contribution of electronic excitations via the Sommerfeld model based on the electronic density of states (DOS) at the Fermi level, the transition temperature is reduced to about 1000 K. Our calculations confirm a recent investigation using the perturbed angular correlation technique,<sup>7</sup> which revealed that an orthorhombic distortion of the  $C11_b$  structure exists in the temperature range from 24 to 1023 K. The calculated phase transition temperature is in reasonable agreement with the experimental value of about 1400 K,<sup>8</sup> considering the applied approximations (such as the harmonic approximation, the neglect of soft modes, and thermal expansion). As illustrated in Fig. 1(b) by the decomposition into internal energy ( $\Delta U = U_{C11_b} - U_{oI6}$ ) and entropy terms [ $-T\Delta S = -T(S_{C11_b} - S_{oI6})$ ], the entropy always favors the  $C11_b$  structure, whereas the internal energy has only little impact on phase stability. Therefore, vibrational entropies are by far the dominant contribution to the structural free energy difference. The phase transition is driven by the vibrational entropy.

Finally, we analyze the instability of the tetragonal structure with respect to orthorhombic distortions from the electronic structure point of view. The total electronic density of states (EDOS) looks rather similar for both structures. Two well separated Pd 4d and Ti 3d related parts can be distinguished. The lower lying fully occupied part of the EDOS is dominated by 4d states of Pd atoms, whereas the higher lying part is mostly due to 3d states of the less electronegative Ti atoms. The most significant differences in the electronic

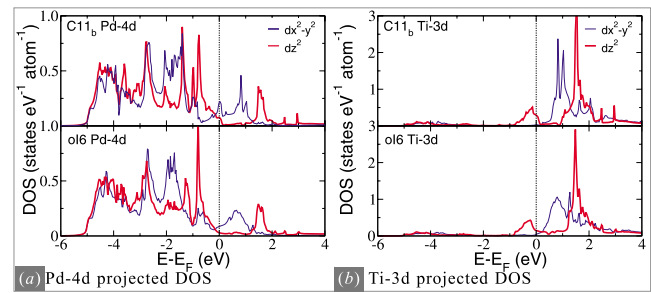


FIG. 2. (Color online) Comparison of the  $d_{x^2-y^2}$  and  $d_{z^2}$  projected EDOS of Pd and Ti in  $C11_b$  and  $oI6$  phases of  $\text{TiPd}_2$ .

structure of the  $C11_b$  and  $oI6$  phases can be observed in the  $d_{x^2-y^2}$  projected DOS of Pd, as is shown in Fig. 2(a). For the  $C11_b$  case, the Fermi level  $E_F$  exactly resides in a peak with a total DOS amounting to  $n(E_F) = 0.8 \text{ states eV}^{-1} \text{ atom}^{-1}$ . Distorting the tetragonal structure to the orthorhombic  $oI6$  structure reduces the total DOS at Fermi energy to  $n(E_F) = 0.5 \text{ states eV}^{-1} \text{ atom}^{-1}$ . Furthermore, the peak of the Pd  $d_{x^2-y^2}$ -like DOS at  $E_F$  vanishes, implying increased electronic stability for the orthorhombic phase.

In summary, the phase stability of  $\text{TiPd}_2$  as a function of temperature is now understood. The low temperature ground state phase is the orthorhombic  $oI6$  structure. It is elastically and vibrationally stable, whereas the tetragonal  $C11_b$  phase is elastically unstable and exhibits a soft mode of imaginary frequency at point X in reciprocal space. At high temperatures above 1000 K, the vibrational entropy drives the transition from the orthorhombic ground state to the dynamically stabilized tetragonal  $C11_b$  phase.

This work was supported by the Austrian Science Fund FWF Project No. P16957. One of the authors (X.-Q.C) also gratefully acknowledges partial support of the National Natural Science Foundation of China (Grant No. 50604004).

\*chenx@ornl.gov

- <sup>1</sup>K. Otsuka and T. Kakeshita, MRS Bull. **27**, 91 (2002).
- <sup>2</sup>B. L. Winn, S. M. Shapiro, R. Erwin, D. L. Schlagel, and T. Lograsso, Appl. Phys. A: Mater. Sci. Process. **74**, S1182 (2002).
- <sup>3</sup>T. Yamamuro, Y. Morizono, J. Honjyo, and M. Nishida, Mater. Sci. Eng., A **438**, 327 (2006).
- <sup>4</sup>L. Schlapbach and A. Züttel, Nature (London) **414**, 353 (2001).
- <sup>5</sup>A. J. Maeland and G. G. Libowitz, J. Less-Common Met. **74**, 295 (1980).
- <sup>6</sup>M. Gupta, R. P. Gupta, and D. J. Singh, Phys. Rev. Lett. **95**, 056403 (2005).
- <sup>7</sup>P. Wodniecki, B. Wodniecka, A. Kulinska, M. Uhrmacher, and K. P. Lieb, J. Alloys Compd. **385**, 53 (2004).
- <sup>8</sup>P. Krautwasser, S. Bhan, and K. Schubert, Z. Metallkd. **59**, 724 (1968).
- <sup>9</sup>H. Okamoto, Phase Diagrams for Binary Alloys (ASM, Materials Park, OH, 2000).
- <sup>10</sup>G. Kresse and J. Hafner, Phys. Rev. B **48**, 13115 (1993); G.

- Kresse and J. Furthmüller, Comput. Mater. Sci. **6**, 15 (1996); Phys. Rev. B **54**, 11169 (1996).
- <sup>11</sup>P. E. Blöchl, Phys. Rev. B **50**, 17953 (1994).
- <sup>12</sup>G. Kresse and D. Joubert, Phys. Rev. B **59**, 1758 (1999).
- <sup>13</sup>J. P. Perdew and Y. Wang, Phys. Rev. B **45**, 13244 (1992).
- <sup>14</sup>H. J. Monkhorst and J. D. Pack, Phys. Rev. B **13**, 5188 (1976).
- <sup>15</sup>K. Parlinski, Z.-Q. Li, and Y. Kawazoe, Phys. Rev. Lett. **78**, 4063 (1997).
- <sup>16</sup>K. Parlinski, PHONON 4.25, as implemented in MedeA, Materials Design Inc., 2005, www.materialsdesign.com
- <sup>17</sup>X.-Q. Chen, W. Wolf, R. Podloucky, and P. Rogl, Phys. Rev. B **71**, 174101 (2005).
- <sup>18</sup>X.-Q. Chen, R. Podloucky, and P. Rogl, J. Appl. Phys. **100**, 113901 (2006).
- <sup>19</sup>X.-Q. Chen, V. T. Witusiewicz, R. Podloucky, P. Rogl, and F. Sommer, Acta Mater. **51**, 1239 (2003).
- <sup>20</sup>W. Ashcroft and N. D. Mermin, Solid State Physics (Holt, Rinehart and Winston, New York, 1976).

- <sup>21</sup>X.-Q. Chen, W. Wolf, R. Podloucky, P. Rogl, and M. Marsman, Phys. Rev. B **72**, 054440 (2005).
- <sup>22</sup>X.-Q. Chen, W. Wolf, R. Podloucky, P. Rogl, and M. Marsman, Europhys. Lett. **67**, 807 (2004).
- <sup>23</sup>J. F. Nye, *Physical Properties of Crystals* (Clarendon, Oxford, 1985).
- <sup>24</sup>D. C. Wallace, *Thermodynamics of Crystals* (Wiley, New York, 1972).
- <sup>25</sup>N. Selhaoui, J. C. Gachon, and J. Hertz, J. Less-Common Met. **154**, 137 (1989).
- <sup>26</sup>N. D. Drummond and G. J. Ackland, Phys. Rev. B **65**, 184104 (2002); M. Sternik and K. Parlinski, J. Chem. Phys. **123**, 204708 (2005).